Cellular and Molecular Biology

Journal homepage: www.cellmolbiol.org

Biocompatible Au-Fe_3O_4 Nanoparticle-based Magnetic Resonance Imaging in the Diagnosis of Liver Tumor

Zhuo Shi[1], Peng Wang[1], Lizhi Xie[2], Xinming Zhao[1*]

[1]*Department of Imaging Diagnosis, National Cancer Center/National Clinical Research Center for Cancer /Cancer Hospital, Chinese Academy of Medical Sciences and Peking Union Medical College, Beijing, 100021, China*

[2]*MR Research China, GE Healthcare, Beijing, 100176, China*

ARTICLE INFO

Original paper

Article history:
Received: September 28, 2021
Accepted: March 22, 2022
Published: March 31, 2022

Keywords:
liver tumor, magnetic resonance imaging, Au-Fe_3O_4, receiver operating characteristic curve

ABSTRACT

The study aimed to analyze the value and significance of magnetic resonance imaging (MRI) using biocompatible Au-Fe_3O_4 nanomaterials in the diagnosis of liver tumors. In this study, 124 patients with liver tumors were selected to perform MRI scanning based on Au-Fe_3O_4 nanoparticles. The coincidence rate between MRI scanning results and pathological examination results, the detection rate of tumor focus between MRI scanning results and CT detection results were analyzed, to evaluate the diagnostic performance of MRI scanning based on Au-Fe_3O_4 nanoparticles. The results showed that in the detection of primary tumors, secondary tumors, and focal nodular hyperplasia, the coincidence rate between MRI scanning results and pathological examination results was high, and Kappa values were all greater than 0.8. Compared with the results of CT, the detection rate of tumor lesions smaller than 1 cm by MRI was significantly higher ($P<0.05$), but there was no significant difference between the two diagnostic methods for tumor lesions larger than 1 cm ($P>0.05$). Additionally, the accuracy, specificity, and sensitivity of MRI in diagnosing liver tumors were 86.81, 84.29, and 77.27, respectively. Clinically, MRI scanning based on Au-Fe_3O_4nanoparticles can provide a practical and effective reference for the differential diagnosis of liver tumors.

DOI: http://dx.doi.org/10.14715/cmb/2022.68.3.8

Introduction

There are benign and malignant liver tumors. Hepatic adenoma, hepatic hemangioma, and focal nodular hyperplasia of the liver are common benign tumors in the clinic, while primary liver cancer and secondary liver cancer are malignant tumors (1). The mortality of liver cancer is very high and the prognosis is poor, seriously threatening the lives of the people in the whole world. China is a heavily-hit country with liver cancer, and its total number of patients with primary liver cancer is more than half the number of patients with primary liver cancer in the world. Each year, approximately 650000 people around the world die of liver cancer, of which half are Chinese. In China, liver cancer has become the biggest killer of tumor-related diseases except for gastric cancer (2-5). Worldwide, it has also become the third leading cause of death of diseases, and its mortality rate is only behind lung cancer and gastric cancer (6). In China, the common high-risk groups of liver cancer mainly include people who drink excessively, patients with hepatitis C virus or hepatitis B virus, patients with nonalcoholic fatty liver disease, patients with liver cirrhosis caused by various reasons, people with a family history of liver cancer, and people who eat aflatoxin-contaminated food for a long time. Additionally, men over 40 years old have a higher risk of suffering from liver cancer (7-9).

In most cases, liver cancer has a relatively hidden onset, lacking obvious specific symptoms in the clinic, and patients can only be diagnosed in the middle and late stages, so most patients miss the best treatment stage. Timely detection and treatment of liver cancer will significantly improve the treatment effect and prognosis of patients. Early diagnosis and timely treatment have become one of the most concerned topics of liver cancer researchers (10-12). At present, examination and diagnosis methods for liver tumors are mainly laboratory diagnosis and imaging examination. Ultrasound, Computed Tomography (CT), and Magnetic Resonance Imaging (MRI) are the most commonly used imaging

*Corresponding author. E-mail: zhaoxinming@cicams.ac.cn

examinations (13,14). Ultrasound examination has many advantages, such as high repeatability, low price, no exposure to harmful radiation, and a non-invasive examination process, which plays an important role in the early screening of liver tumors. However, due to the influence of factors such as the location and size of the lesion, instrument resolution, and echo characteristics, many false negatives and false positives often appear in the examination results. Besides, it cannot differentiate and diagnose different types of liver cancer (15,16). CT can overcome the limitations of ultrasound diagnosis, judge the basic information such as the location and size of the lesion, and at the same time make a differential diagnosis for various types of liver cancer with typical features, but there are still some obstacles in CT examination and diagnosis when the features are not typical (17-20).

Clinically, many studies have shown that MRI examination has high resolution and plays an important role in the diagnosis of liver tumors. MRI can accurately display the images of liver cancer to show indiscernible tissue lesions (21-23). Therefore, in recent years, MRI has become the most important auxiliary examination method in the clinic because of its advantages of no harmful radiation, non-invasiveness, high tissue resolution, and accurate imaging (24). Nanoparticles can improve the resolution between tumor and normal tissues by their specific binding with glioma cells, and importantly, they have no toxic or side effects on normal tissue (25-27). Fe_3O_4 nanoparticles play an important role in MRI because of their high saturation magnetic susceptibility and good magnetic properties (28). Au-Fe_3O_4 composite nanoparticles are a complex formed by the combination of nano-gold and Fe_3O_4 and have the characteristics of both Au and Fe_3O_4. The application of Au-Fe_3O_4 composite nanoparticles in MRI detection has attracted researchers' attention for the early diagnosis of tumors. The development of a new multi-functional nanoparticle platform assists the physician in the early accurate diagnosis of tumor cells, thus further improving the accuracy and precision of early diagnosis of cancer (29).

In this study, 124 patients with liver tumors were selected for MRI scanning based on Au-Fe_3O_4 nanoparticles to analyze the value and significance of MRI information using biocompatible Au-Fe_3O_4 nanomaterials in the diagnosis of liver tumors. The coincidence rate between MRI scanning results and pathological examination results, the detection rate of tumor focus between MRI scanning results and CT detection results were analyzed, to evaluate the diagnostic performance of MRI scanning based on Au-Fe_3O_4 nanoparticles in the diagnosis of liver tumors.

Materials and methods

Research subjects

In this study, 124 liver tumor patients admitted to the hospital from January 10, 2020, to May 10, 2021, were selected for MRI scanning based on Au-Fe_3O_4 nanoparticles. This study had been approved by the Medical Ethics Committee of the Hospital, and the family members of patients knew about this study and signed the informed consent form.

Inclusion criteria: I patients diagnosed as having liver tumors according to diagnostic criteria; II patients who had signed the informed consent form; and III patients without contraindications for MRI examination.

Exclusion criteria: I patients with mental illness who can't cooperate with the study; II. patients allergic to related drugs; III. Patients with other serious basic diseases; and IV patients whose family members did not agree and did not sign the informed consent form.

Basic information collection

A total of 124 patients with liver tumors participated in this study, ranging in age from 20 to 76 years old, with an average age of 65.23$\pm$5.9 years old. Among them, there were 69 male patients and 55 female patients. Of all patients, there were 79 patients with primary liver cancer, 38 patients with secondary liver cancer, and 7 patients with focal nodular hyperplasia of the liver. In patients with secondary liver cancer, the primary lesions were colon cancer, lung cancer, stomach cancer, pancreatic cancer, breast cancer, cervical cancer, and rectal cancer. The specific number of patients with various liver tumors was shown in Figure 1.

Imaging examination

Siemens Avanto Dot 1.5T (Germany) was used for MRI scanning. Toshiba scanner was used for CT scanning. The patient was in a supine position for

image acquisition. Three ways of the plain scan, enhanced scan, and Diffusion-Weighted Imaging (DWI) scan were performed. Au-Fe_3O_4 nanoparticles were used as the contrast agent to observe and record the signal characteristics. The specific scanning parameters were shown in Figure 2 below.

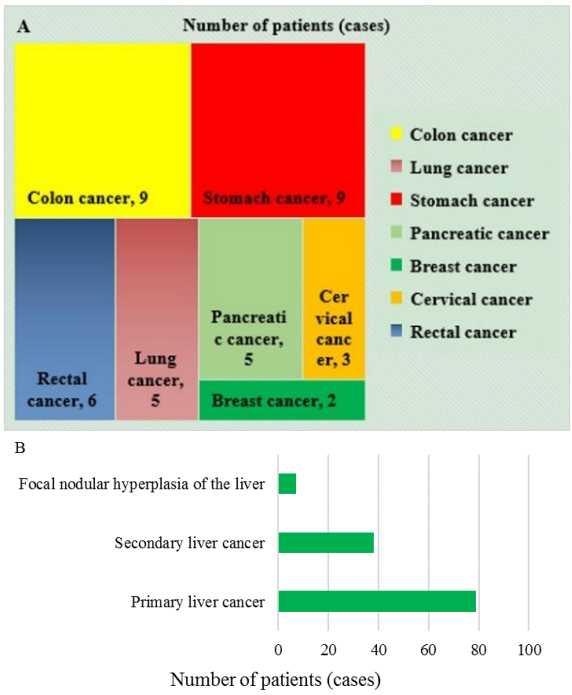

Figure 1. Basic information of the patients. Note: Figure 1A: distribution of different liver tumor types; Figure 1B: distribution of different primary lesions in patients of secondary hepatocellular carcinoma. 1. Basic information about the patients.

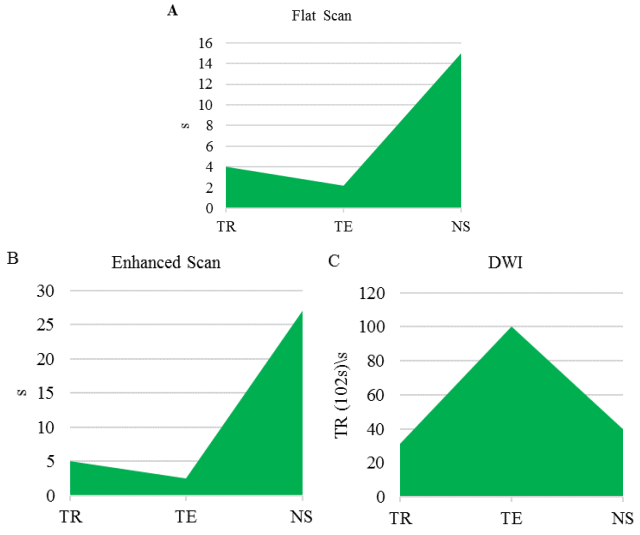

Figure 2. MRI parameters. Note: Figure 2A: parameter information of plain scanning; Figure 2B: parameter information of enhanced scanning; Figure 2C: parameter information of DWI

Evaluation index

The coincidence rate between pathological results and MRI results based on Au-Fe_3O_4 nanoparticles and the Kappa value were calculated. In this study, a total of 148 liver tumor lesions were detected in 124 patients, and the detection rate of liver tumor lesions by MRI and CT was compared and analyzed retrospectively. With pathological diagnosis results as the reference standard, three common indexes were selected to evaluate the ability of MRI based on Au-Fe_3O_4 nanoparticles to diagnose liver tumors, namely, Accuracy, Specificity, and Sensitivity, expressed as follows.

$$Accuracy = \frac{TA + TB}{TA + NA + TB + NB} \quad (1)$$

$$Specificity = \frac{TB}{NA + TB} \quad (2)$$

$$Sensitivity = \frac{TA}{NB + TA} \quad (3)$$

Where TA is truly positive, which means that the diagnosis result is positive, and it is positive; TN means true negative, indicating that the diagnosis result is negative and it is negative; FP is false positive, which means that the diagnosis result is positive, but it is negative; and FB is a false negative, which means that the actual result is positive but the diagnosis result is negative.

The receiver operating characteristic curve (ROC) curve is used to express the diagnostic ability of MRI for liver tumors, and the area under the ROC curve (AUC) is determined according to ROC.

Statistical methods

SPSS software is used to statistically analyze the data, and the Kappa test is used to evaluate the consistency between MRI and pathological diagnosis. When Kappa value <0.4, the consistency is poor; when 0.4<Kappa value<0.75, the consistency is average; and when kappa value >0.75, the consistency between MRI and pathological diagnosis is high. The T-test is used for measurement data, and Chi-square ($\chi 2$) test is for count data. $P<0.05$ indicates a statistical difference.

Results and discussion

MRI imaging results of patients

Figure 3 showed the MRI images of 6 patients with different primary liver tumors, showing the liver tumor lesions in different positions with different

sizes. The MRI images based on Au-Fe_3O_4nanoparticles can detect tiny lesions less than 1 cm.

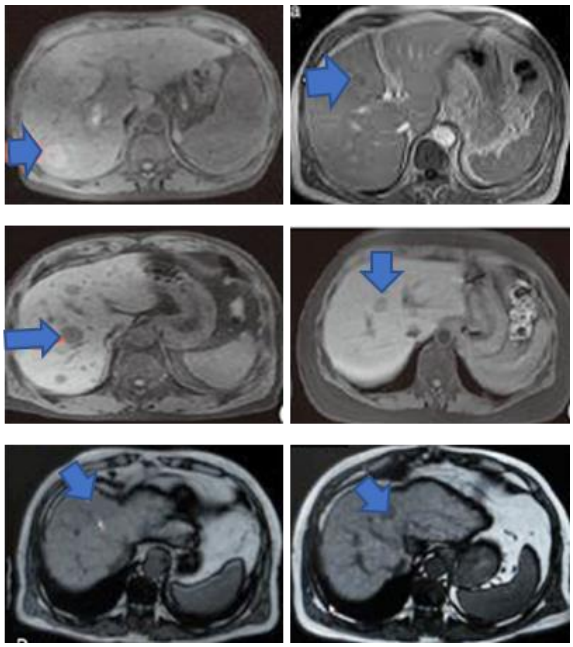

Figure 3. MRI images of liver tumor patients.

Coincidence rate for primary liver cancer

The coincidence rate between MRI and pathological diagnosis of primary liver cancer was analyzed by the Kappa test. The results showed that the coincidence rate was 96.2% and the Kappa value was > 0.8. The two detection methods were highly consistent in the diagnosis of primary liver cancer, and the specific number was shown in Figure 4.

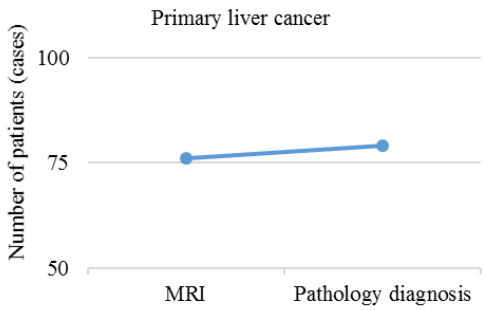

Figure 4. Coincidence rate of MRI detection of primary liver cancer.

Coincidence rate for secondary liver cancer

The coincidence rate between MRI and pathological diagnosis of secondary liver cancer was analyzed by the Kappa test. The results showed that the coincidence rate was 94.74% and the Kappa value was > 0.8. The two detection methods were highly consistent in the diagnosis of primary liver cancer, and the specific number was shown in Figure 5.

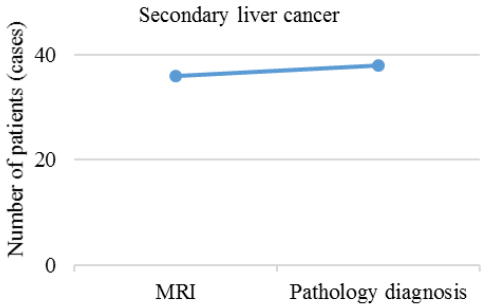

Figure 5. Coincidence rate of MRI detection of secondary liver cancer.

Coincidence rate for focal nodular hyperplasia of the liver

Kappa test was performed to analyze the coincidence rate between MRI and pathological diagnosis of focal nodular hyperplasia of the liver. The results showed that the coincidence rate was 85.71%, and the Kappa value was> 0.8. The two detection methods were highly consistent in the diagnosis of focal nodular hyperplasia of the liver, and the specific number was shown in Figure 6.

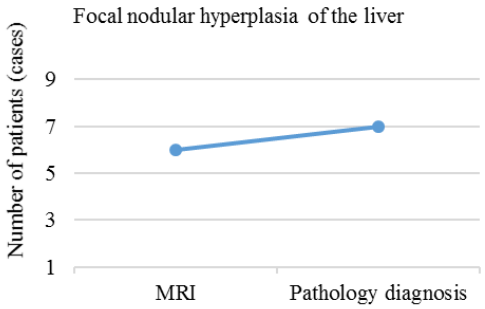

Figure 6. Coincidence rate of MRI detection of hepatic focal nodular hyperplasia.

Comparison of detection rates of different lesions

The detection rates of 148 liver tumor lesions by MRI and CT were compared. The results showed that the detection rate of MRI was significantly higher than that of CT for lesions with a size of less than 1 cm (P<0.05), while there was no significant statistical difference between the two methods for lesions with a size of 1-5 cm (P>0.05). The specific results were shown in Figure 7.

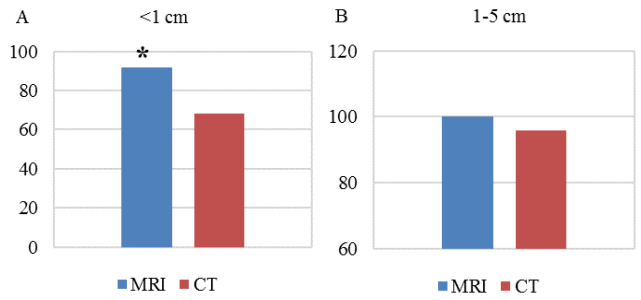

Figure 7. Detection rates of different lesions. Note: * indicated significant differences, $P<0.05$; Figure 7A: <1 cm lesion; Figure 7B: 1-5 cm lesion

Diagnostic performance of MRI examination

By calculating the accuracy, specificity and sensitivity, it was found that the accuracy, specificity, and sensitivity of MRI in diagnosing liver tumors were 94.32, 93.23, and 85.23, respectively, and the specific results were shown in Figure 8.

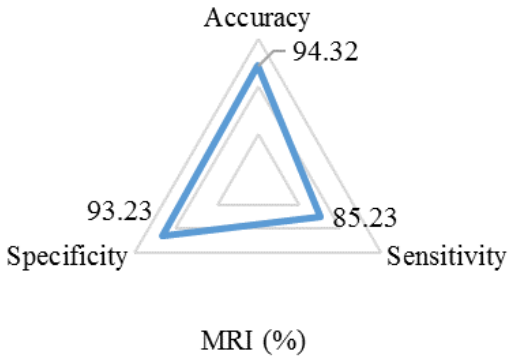

Figure 8. Performance of MRI in the diagnosis of liver tumors.

The ROC curve was drawn according to the specificity and sensitivity of MRI in diagnosing liver tumors, as shown in Figure 9. Meanwhile, AUC was determined to be 0.889 according to ROC.

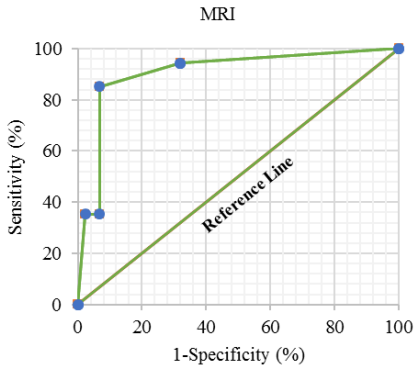

Figure 9. ROC curve of Au-Fe_3O_4 nanoparticle-based MRI in the diagnosis of liver tumor.

In recent years, the incidence of liver tumors has been rising continuously, and it has become one of the first three deadly cancers. Its location is insidious, its clinical manifestations are not obvious, and there are no specific symptoms. Often, patients can only be diagnosed at the late stage, which leads to poor treatment effects and prognosis. Therefore, early diagnosis and timely treatment of liver tumors are particularly important (30) MRI examination has a high resolution for the diagnosis of liver tumors. MRI can accurately display images of liver cancer to show the tissue lesions that cannot be determined (31). Au-Fe_3O_4 nanoparticles have good biocompatibility and chemical stability. It is easy to synthesize and modify, so they are widely used in the biomedical field, especially in the early diagnosis of cancer, which has attracted the attention of many researchers (32). In order to analyze the value and significance of MRI based on biocompatible Au-Fe_3O_4 nanoparticles in the diagnosis of liver tumors, this study selected 124 patients with liver tumors to perform MRI scanning based on Au-Fe_3O_4 nanoparticles. Then, the coincidence rate between MRI scanning results and pathological examination results was calculated, and MRI scanning and CT detection were compared for the detection rate of tumor focus, to evaluate the diagnostic performance of MRI scanning based on Au-Fe_3O_4 nanoparticles for liver tumors.

Clinically, focal nodular hyperplasia of the liver is a common benign tumor, while primary liver cancer and secondary liver cancer are malignant tumors. The coincidence rate between MRI and pathological diagnosis of primary liver cancer was analyzed by the Kappa test. The results showed that the coincidence rate was 96.2% and the Kappa value was > 0.8. The two detection methods had high consistency in the diagnosis of primary liver cancer. The coincidence rate between MRI and pathological diagnosis of secondary liver cancer was analyzed. The results showed that the coincidence rate was 94.74% and the Kappa value was > 0.8. The two detection methods were highly consistent in the diagnosis of primary liver cancer. Kappa test was used to analyze the coincidence rate between MRI and pathological diagnosis of liver focal nodular hyperplasia. The results showed that the coincidence rate was 85.71% and the Kappa value was > 0.8. The two detection methods were highly consistent in the diagnosis of

liver focal nodular hyperplasia, which indicated that MRI based on Au-Fe_3O_4 nano-materials was effective in the diagnosis of different kinds of liver tumors. The detection rate of 148 liver tumor lesions by MRI and CT was analyzed. The results showed that the detection rate of MRI was significantly higher than that of CT for tumors with a size of less than 1 cm (P<0.05), but there was no significant statistical difference between the two methods for tumors with a size of 1-5 cm (P>0.05), which indicated that MRI imaging based on Au-Fe_3O_4 nanoparticles was superior to CT in the diagnosis of small liver tumor lesions. By calculating the accuracy, specificity, and sensitivity, it was found that the accuracy, specificity, and sensitivity of MRI in diagnosing liver tumors were 94.32, 93.23, and 85.23, respectively. According to the specificity and sensitivity of MRI in diagnosing liver tumors, the ROC curve was drawn, and AUC was 0.889. Some studies have found that when Au-Fe_3O_4 nanomaterials were applied to mouse models, they can increase the resolution of mouse liver tumor tissue. In addition, due to its chemical and colloidal stability, the complex has great potential in the field of MRI diagnosis of tumors, which was in good agreement with the results of this study (33). To sum up, in addition to therapeutic applications of Au and Fe_3O_4 NPs (34-38), MRI based on Au-Fe_3O_4 nanomaterials has great application value in the diagnosis of liver tumors.

Conclusions

In this study, 124 patients with liver tumors were selected for MRI scanning based on Au-Fe_3O_4 nanoparticles. The coincidence rate between MRI scanning results and pathological examination results, the detection rate of tumor focus between MRI scanning results and CT detection results were analyzed, to evaluate the diagnostic performance of MRI scanning based on Au-Fe_3O_4nanoparticles. It was found that MRI based on Au-Fe_3O_4 nanomaterials was effective in the diagnosis of different kinds of liver tumors, such as primary liver cancer, secondary liver cancer, and focal nodular hyperplasia. In addition, the diagnostic ability of MRI based on Au-Fe_3O_4 nanomaterials was better than that of CT diagnosis, and the accuracy, specificity, and sensitivity of MRI were higher in the diagnosis of liver tumors, which could provide a reference for clinical diagnosis of liver tumors. The deficiency of this study lies in the single source of research subjects, which does not have wide applicability. In the future study, multi-site, multi-type, and multi-sample analysis and research will be considered. Meanwhile, a healthy control group can be set for comparative analysis. In conclusion, the study provides an effective reference for the application of MRI based on Au-Fe_3O_4 nanomaterial in liver tumor diagnosis.

Acknowledgments

Not applicable.

Conflict interest

The authors declare that they have no conflict of interest.

References

1. Anwanwan D, Singh SK, Singh S, Saikam V, Singh R. Challenges in liver cancer and possible treatment approaches. Biochim Biophys Acta Rev Cancer. 2020 Jan;1873(1):188314.
2. Xu F, Jin T, Zhu Y, Dai C. Immune checkpoint therapy in liver cancer. J Exp Clin Cancer Res. 2018 May 29;37(1):110.
3. Yang WS, Zeng XF, Liu ZN, Zhao QH, Tan YT, Gao J, Li HL, Xiang YB. Diet and liver cancer risk: a narrative review of epidemiological evidence. Br J Nutr. 2020 Aug 14;124(3):330-340.
4. Wang C, Vegna S, Jin H, Benedict B, Lieftink C, Ramirez C, de Oliveira RL, Morris B, Gadiot J, Wang W, du Chatinier A, Wang L, Gao D, Evers B, Jin G, Xue Z, Schepers A, Jochems F, Sanchez AM, Mainardi S, Te Riele H, Beijersbergen RL, Qin W, Akkari L, Bernards R. Inducing and exploiting vulnerabilities for the treatment of liver cancer. Nature. 2019 Oct;574(7777):268-272.
5. Orcutt ST, Anaya DA. Liver Resection and Surgical Strategies for Management of Primary Liver Cancer. Cancer Control. 2018 Jan-Mar;25(1):1073274817744621.
6. Fu J, Wang H. Precision diagnosis and treatment of liver cancer in China. Cancer Lett. 2018 Jan 1;412:283-288.
7. Wang H, Lu Z, Zhao X. Tumorigenesis, diagnosis, and therapeutic potential of exosomes in liver cancer. J Hematol Oncol. 2019 Dec 9;12(1):133.

8. Kawaguchi K, Kaneko S. Notch Signaling and Liver Cancer. Adv Exp Med Biol. 2021;1287:69-80.
9. Bresnahan E, Ramadori P, Heikenwalder M, Zender L, Lujambio A. Novel patient-derived preclinical models of liver cancer. J Hepatol. 2020 Feb;72(2):239-249.
10. Shi JF, Cao M, Wang Y, Bai FZ, Lei L, Peng J, Feletto E, Canfell K, Qu C, Chen W. Is it possible to halve the incidence of liver cancer in China by 2050? Int J Cancer. 2021 Mar 1;148(5):1051-1065.
11. Vempati RK, Malla RR. Autophagy-Induced Drug Resistance in Liver Cancer. Crit Rev Oncog. 2020;25(1):21-30.
12. Cheng Z, Wei-Qi J, Jin D. New insights on sorafenib resistance in liver cancer with correlation of individualized therapy. Biochim Biophys Acta Rev Cancer. 2020 Aug;1874(1):188382.
13. Hu S, Gan W, Qiao L, Ye C, Wu D, Liao B, Yang X, Jiang X. A New Prognostic Algorithm Predicting HCC Recurrence in Patients With Barcelona Clinic Liver Cancer Stage B Who Received PA-TACE. Front Oncol. 2021 Oct 21;11:742630.
14. Inoue N, Kawabata H, Miyata M. A Case of Advanced Gastric Cancer With Multiple Liver Metastases in Which Hypoglycemic Symptoms Triggered the Diagnosis. Cureus. 2021 Sep 30;13(9):e18407.
15. Hakobyan K, Gaddam M, Ojinnaka U, Ahmed Z, Kannan A, Quadir H, Mostafa JA. Contrast-Enhanced Ultrasound as a Main Radiological Diagnostic Method for Primary Liver Neoplasms and Hemangiomas. Cureus. 2021 Sep 25;13(9):e18288.
16. Ye C, Zhang W, Pang Z, Wang W. Efficacy of liver cancer microwave ablation through ultrasonic image guidance under deep migration feature algorithm. Pak J Med Sci. 2021;37(6):1693-1698.
17. Wang X, Liu L, Ma N, Zhao X. Computed Tomography Image Feature under Intelligent Algorithms in Diagnosing the Effect of Humanized Nursing on Neuroendocrine Hormones in Patients with Primary Liver Cancer. J Healthc Eng. 2021 Oct 6;2021:4563100.
18. Nadarevic T, Giljaca V, Colli A, Fraquelli M, Casazza G, Miletic D, Štimac D. Computed tomography for the diagnosis of hepatocellular carcinoma in adults with chronic liver disease. Cochrane Database Syst Rev. 2021 Oct 6;10(10):CD013362.
19. Gao R, Zhao S, Aishanjiang K, Cai H, Wei T, Zhang Y, Liu Z, Zhou J, Han B, Wang J, Ding H, Liu Y, Xu X, Yu Z, Gu J. Deep learning for differential diagnosis of malignant hepatic tumors based on multi-phase contrast-enhanced CT and clinical data. J Hematol Oncol. 2021 Sep 26;14(1):154.
20. Kido H, Kato S, Funahashi K, Shibuya K, Sasaki Y, Urita Y, Hori M, Mizumura S. The metabolic parameters based on volume in PET/CT are associated with clinicopathological N stage of colorectal cancer and can predict prognosis. EJNMMI Res. 2021 Sep 6;11(1):87.
21. Ma YQ, Wen Y, Liang H, Zhong JG, Pang PP. Magnetic resonance imaging-radiomics evaluation of response to chemotherapy for synchronous liver metastasis of colorectal cancer. World J Gastroenterol. 2021 Oct 14;27(38):6465-6475.
22. Moctezuma-Velázquez C, Lewis S, Lee K, Amodeo S, Llovet JM, Schwartz M, Abraldes JG, Villanueva A. Non-invasive imaging criteria for the diagnosis of hepatocellular carcinoma in non-cirrhotic patients with chronic hepatitis B. JHEP Rep. 2021 Sep 16;3(6):100364.
23. Panvini N, Dioguardi Burgio M, Sartoris R, Maino C, Van Wettere M, Plessier A, Payence A, Rautou PE, Ladouceur M, Vilgrain V, Ronot M. MR imaging features and long-term evolution of benign focal liver lesions in Budd-Chiari syndrome and Fontan-associated liver disease. Diagn Interv Imaging. 2021 Oct 12:S2211-5684(21)00198-4.
24. Stollmayer R, Budai BK, Tóth A, Kalina I, Hartmann E, Szoldán P, Bérczi V, Maurovich-Horvat P, Kaposi PN. Diagnosis of focal liver lesions with deep learning-based multi-channel analysis of hepatocyte-specific contrast-enhanced magnetic resonance imaging. World J Gastroenterol. 2021 Sep 21;27(35):5978-5988.
25. Klein S, Distel LVR, Neuhuber W, Kryschi C. Caffeic Acid, Quercetin and 5-Fluorocytidine-Functionalized Au-Fe3O4 Nanoheterodimers for X-ray-Triggered Drug Delivery in Breast Tumor Spheroids. Nanomaterials (Basel). 2021 Apr 29;11(5):1167.
26. Katifelis H, Lyberopoulou A, Vityuk N, Grammatikaki M, Pylypchuk I, Lazaris F, Storozhuk L, Kouloulias V, Gazouli M. In vitro effect of hyperthermic Ag and Au Fe3O4 nanoparticles in cancer cells. J BUON. 2020 Mar-Apr;25(2):1212-1218.
27. Cai J, Miao YQ, Li L, Fan HM. Facile Preparation of Gold-Decorated Fe_3O_4 Nanoparticles for CT and MR Dual-Modal

Imaging. Int J Mol Sci. 2018 Dec 14;19(12):4049.
28. Sun W, Huang S, Zhang S, Luo Q. Preparation, Characterization and Application of Multi-Mode Imaging Functional Graphene Au-Fe3O4 Magnetic Nanocomposites. Materials (Basel). 2019 Jun 19;12(12):1978.
29. Liu D, Li X, Chen C, Li C, Zhou C, Zhang W, Zhao J, Fan J, Cheng K, Chen L. Target-specific delivery of oxaliplatin to HER2-positive gastric cancer cells in vivo using oxaliplatin-au-fe3o4-herceptin nanoparticles. Oncol Lett. 2018 May;15(5):8079-8087.
30. Han H, Zhou S, Chen G, Lu Y, Lin H. ABAT targeted by miR-183-5p regulates cell functions in liver cancer. Int J Biochem Cell Biol. 2021 Nov 3:106116.
31. Carbonell G, Kennedy P, Bane O, Kirmani A, El Homsi M, Stocker D, Said D, Mukherjee P, Gevaert O, Lewis S, Hectors S, Taouli B. Precision of MRI radiomics features in the liver and hepatocellular carcinoma. Eur Radiol. 2022 Mar;32(3):2030-2040.
32. Wang X, Chen L, Ge J, Afshari MJ, Yang L, Miao Q, Duan R, Cui J, Liu C, Zeng J, Zhong J, Gao M. Rational Constructed Ultra-Small Iron Oxide Nanoprobes Manifesting High Performance for T1-Weighted Magnetic Resonance Imaging of Glioblastoma. Nanomaterials (Basel). 2021 Oct 2;11(10):2601.
33. Xu F, Li X, Chen H, Jian M, Sun Y, Liu G, Ma L, Wang Z. Synthesis of heteronanostructures for multimodality molecular imaging-guided photothermal therapy. J Mater Chem B. 2020 Nov 18;8(44):10136-10145.
34. Sami A, Naqvi SS, Qayyum M, Rao AR, Sabitaliyevich UY, Ahmad MS. Calcium based siRNA coating: a novel approach for knockdown of HER2 gene in MCF-7 cells using gold nanoparticles. Cellular and Molecular Biology. 2020 Sep 30;66(6):105-11.
35. Alavi M, Karimi N. Ultrasound assisted-phytofabricated Fe3O4 NPs with antioxidant properties and antibacterial effects on growth, biofilm formation, and spreading ability of multidrug resistant bacteria, Artif Cells Nanomed Biotechnol. 2019 47:1, 2405-2423.
36. Zare, M., Soltanzadeh, H., Narimani, R. Plasma Level of miRNA-7, miRNA-409 and miRNA-93 as Potential Biomarkers for Colorectal Cancer. J Genet Resour 2019; 5(1): 9-16. doi: 10.22080/jgr.2019.15896.1125.
37. Khaledian S, Abdoli M, Shahlaei M, Behbood L, Kahrizi D, Arkan E, Moradi S. Two-dimensional nanostructure colloids in novel nano drug delivery systems. Colloids Surf A Physicochem Eng Asp 2020 Jan 20;585:124077. doi: 10.1016/j.colsurfa.2019.124077.
38. Zaki EI, El-Seedy AS, Kelada IP, Sharafeldin NA, Abdel Mouaty HM, Ramadan HS. Impact of citrate- and chitosan-capped gold nanoparticles on the liver of Swiss albino mice: Histological and cyto-genotoxic study. Cell Mol Biol (Noisy-le-grand). 2019 Jun 30;65(5):9-23.